Three-Dimensional Optimization of a Gas Turbine Disk and Blade Attachment

R.G. Alderson,* M.A. Tani,† D.J. Tree,‡
Garrett AiResearch Manufacturing Company, Phoenix, Ariz.
and
R. J. Hill§
Air Force Aero Propulsion Laboratory, Wright-Patterson Air Force Base, Ohio

A new three-dimensional finite-element stress simulation is described and applied to design optimization of a turbine disk/blade attachment. Isoparametric elements are employed, with the standard elements being a general parabolic conoid and a variable thickness triangle. The stress field obtained is improved with the use of a conjugate approximation. A parametric study is used to select optimum attachment geometry. The analysis model includes complex airfoil geometry and a nonzero broach angle.

I. Introduction

THE United States Air Force currently is conducting in-house analyses of developmental aircraft gas turbine engine components in order to be assured of a "best" buy in terms of mission capability, durability, and cost. Additionally, the Air Force is analyzing proposed design modifications to existing in-service engine hardware on a function, safety, and life-cycle cost basis.

In order to accomplish these types of analyses in the most cost-effective manner, the Air Force has funded the development of computer stress analysis techniques specifically oriented toward discrete analysis of engine rotating components. This stress-analysis capability is versatile and eventually will find great utilization in the aircraft gas turbine engine industry as a tool for design optimization and analysis.

The design of a disk and blade attachment is a vital consideration in the development of modern high-speed and high-performance turbine engines. Although the design problem deals with a complex three-dimensional geometry, much of today's design activity relies on two-dimensional approaches. It is well established that the finite-element method provides the designer with better design data than were available previously, but limiting this method to a two-dimensional approach deprives the designer of information that can result in a better design. It is the intent of this paper to describe a practical three-dimensional approach and to demonstrate its application to the design of a disk and blade attachment. It will be shown that some aspects of the design must be evaluated by a fully three-dimensional approach, but that simplified two-dimensional representations continue to play an important part in the design process.

In the approach described, finite-element models in two and three dimensions were applied to the study of a typical axial-flow compressor disk with an inserted blade. All stress analyses utilized the finite-element computer program family ISOPDQ,[1] specifically developed for analysis of high-performance turbine engine disk and blade components. Programs of this family emphasize user convenience, permitting rapid detailed modeling and accurate assessment of stress distributions in engine components.

The primary three-dimensional element employed is a parabolic conoid, based on isoparametric interpolation functions which permit quadratic variation in one parametric coordinate and linear variation in the remaining two. Use of isoparametric interpolation functions, introduced by Ergatoudis, et al.,[2] is considered to furnish the simplest formulation consistent with a realistic representation of engine components. The two-dimensional analysis employed a simple isoparametric quadrilateral.

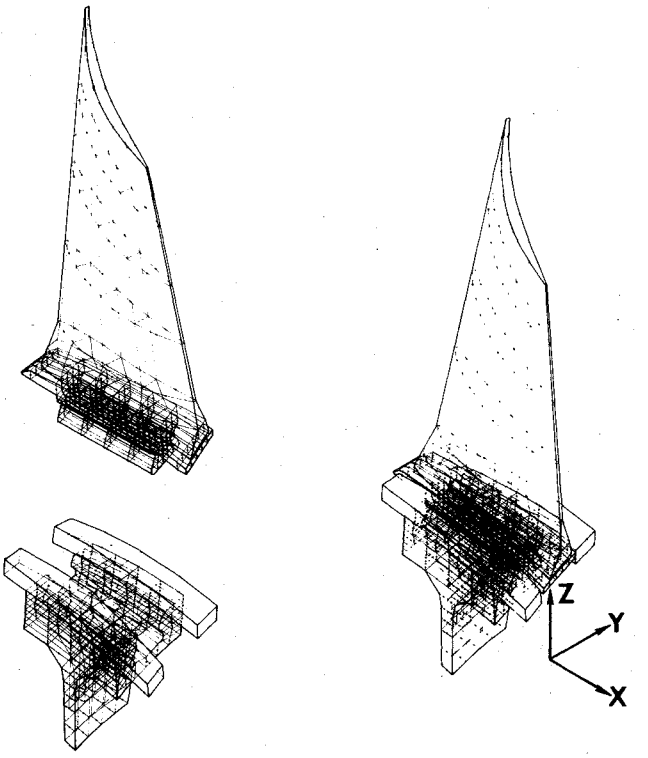

Fig. 1 Blade/disk model from ISO3DQ for a compressor blade at 38° broach angle.

Presented as Paper 75-1312 at the AIAA/SAE 11th Propulsion Conference, Anaheim, Calif., Sept. 29–Oct. 1, 1975; submitted Dec. 5, 1975; revision received March 22, 1976. This study was based on stress analysis techniques developed by AiResearch under Air Force Aero Propulsion Laboratory Contract No. F33615-74-C-2012, "Turbine Engine Components Stress Simulation Program." The authors are indebted to J. W. Harvey for his assistance in theoretical aspects of this study, and to D. H. Cooke for editorial assistance in the preparation of this paper for publication.

Index category: Structural Design, Optimal.

*Senior Engineering Specialist.
†Computing Specialist.
‡Supervisor, Mechanical Component Design.
§Project Engineer.

Special techniques designed to extract the most accurate information available from the finite-element models are incorporated in the stress simulations. Stress calculations are based on conjugate approximations, well demonstrated by Oden and Brauchli,[3] to provide the most accurate stress field available. Computationally, it is the authors' experience that this technique is remarkably economical as well as elegant, yielding a degree of accuracy well beyond that obtainable by comparable investment in model refinement.

For airfoil simulations the simple interpolation functions used in finite-element formulations can lead to significant overestimation of the contribution of shearing detrusion to the element stiffness. This problem has been treated by Wempner, et al.,[4] Doherty, et al.,[5] Zienkiewicz, et al.,[6] and Pawsey and Clough.[7] The phenomenon was denoted as "parasitic shear" by Zienkiewicz and co-workers. The corrective method of selective integration (suggested by the referenced works) has been used with excellent results.

Extensive use has been made of the linear constraints (Lagrange multiplier) technique generalized by Greene[8] and applied to various structural problems by Pian,[9] Anderheggen,[10] Harvey and Kelsey,[11] and others. The particular applications in this work are in the interfacing of substructures with nonmatching nodal meshes and in the enforcement of cyclosymmetric boundary conditions. The first application provides a stable equilibrated interface with pointwise compatibility, whereas the second permits the complete representation of a repetitively symmetric engine component by the finite-element model of a single segment. A further application of the constraint technique is in the representation of the contract surface mating of the dovetail attachment and its recess.

II. Analytical Approach

An analysis method that takes full account of the complex three-dimensional nature of the blade, disk, and attachment area has the potential for providing insight beyond the capabilities of the most refined two-dimensional empirical evaluation. No assumption is required as to the effect of broach angle or load distribution; and the effects of normal disk stress conditions, rim thickness, and blade lean, for example, may be assessed for significance.

The major disadvantage with three-dimensional techniques in comparison with two-dimensional methods is the sharp increase in central processor time required to obtain a solution. For this reason, the authors feel that an effective welding of two- and three-dimensional methods will present real advantages during the design process.

The individual advantages of the two programs were exploited by an analysis plan that relied on both. The initial step was a full three-dimensional analysis of the basic configuration. Appropriate loads and displacements were selected to be used as boundary conditions for the two-dimensional parametric study. Following development of an improved broach contour, a second three-dimensional analysis was conducted on a design incorporating the improved contour. This design also included a wider rim to achieve better load distribution along the broach.

Throughout the study, the primary design criterion was the maximum effective stress in the disk fillet area, effective stress being defined as

$$\sigma_E = \sqrt{2}/2)^{1/2} \sqrt{(\sigma_1 - \sigma_2)^2 + (\sigma_1 - \sigma_3)^2 + (\sigma_2 - \sigma_3)^2}$$

where σ_1, σ_2, σ_3 are principal stresses.

Geometric Modeling

The geometric modeling process divides a system to be modeled into a few natural blocks, large or small, with each block containing several finite elements. The blocks are defined by one or more plane sections, with interpolation employed to develop a three-dimensional block from the plane sections.

A model generated by this procedure is shown in Fig. 1. The global X axis is the axis of rotation; the Z axis is the airfoil stacking axis; and the Y axis is the right-handed tri-normal. The positive X direction is aft. The blade is formed by joining five separate blocks of elements together, whereas the disk is obtained by joining six separately formed blocks. The junctures between building blocks are accomplished by linear constraint equations or by commonality of nodes.

A single blade and a corresponding disk segment were modeled. The "pie-cut" shaped disk segment has complex boundary surfaces formed by radial lines originating at the axis of rotation and following the 38° broach angle at the rim. The resultant surface is a hyperbolic parabaloid formed by straight line generators and four straight line boundaries.

The following assumptions were made during the geometric modeling:

1) The contact region of both disk and blade was well defined for adequate stress-state simulation.

2) An accurate representation of blade loading and stiffness was required, but close simulation of blade stress was not essential. Thus, a crude model of the airfoil and root was deemed sufficient. The linear constraint of the airfoil to the platform was concerned mainly with load transfer.

3) The lower portion of the disk was modeled to provide a suitable restraint for the rim area, and an accurate simulation of the stress at the interface and at the inner radius was not required.

4) The overhanging portions of the disk rim and blade platform were modeled crudely to provide mass and stiffness representation only, with no intention of obtaining usable stresses.

Boundary Condition Simulation

At the inner boundary of the disk segment, a displacement was prescribed in the radial direction, consistent with values obtained from axisymmetric finite-element analysis of the disk. Numerically, a displacement condition at a node is handled more efficiently than a stress condition.

At the side surfaces of the disk segment, a cyclosymmetric condition was established. Cyclosymmetry may be defined as a class of deformation wherein repetitive geometrical subdivisions of a structure behave as cyclic images. The disk segment has this property, even though the blade loading is not symmetric with respect to the local subdivision.

At the interface between disk and blade, much care is required in obtaining realistic boundary conditions. It is tempting to simulate high friction because of high contact stresses by defining nodes at the disk and blade contact surface to have identical displacements. Under certain conditions, however, this may provide a tension tie across the blade shank and give a completely erroneous stress state. The unrealistic tension tie occurs when part of the blade contact area should lose contact with the disk, but is prevented from doing so by the identical displacement constraint. In the present analysis, this effect was minimized by permitting free motion between disk and blade in the plane of the contact surface, with zero relative motion normal to these surfaces. Effective handling of friction must await development of a program feature that simulates the "compression only" characteristic of contacting surfaces.

In employing a two-dimensional technique for the analysis of the three-dimensional segment of the blade-disk shown in Fig. 2, it is recognized that different conditions obtain at the forward and aft faces compared to the central plane. The geometry and cyclosymmetry conditions require at least two analyses: for a plane where no disk supports the rim, and for a central plane. Dashed lines in Fig. 2 indicate these planes.

Two-Dimensional Analysis

The process of identifying a candidate redesign configuration was expedited through the use of two-dimensional

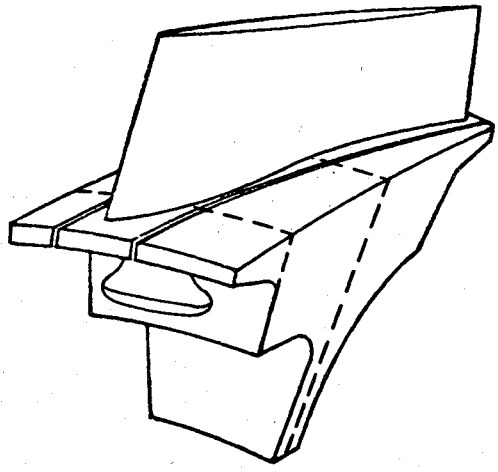

Fig. 2 A typical section of a compressor disk at a dovetail slot employed for three-dimensional analysis. (Dashed lines represent planes used for two-dimensional analysis.)

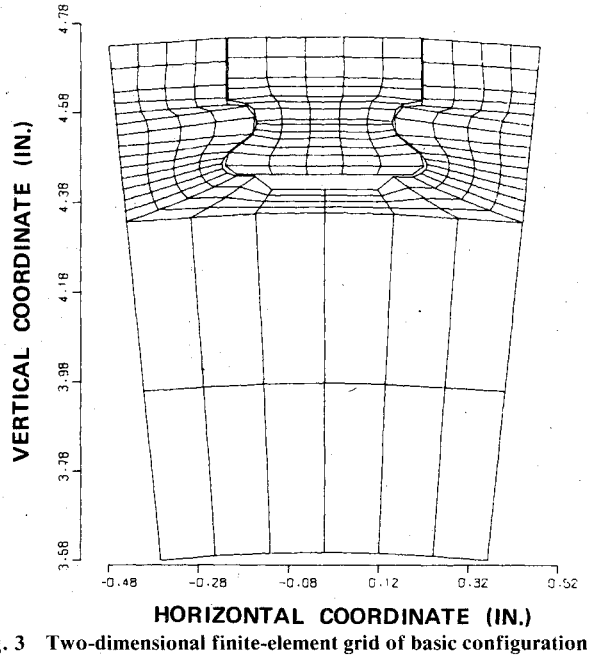

Fig. 3 Two-dimensional finite-element grid of basic configuration at midplane.

finite-element models to obtain a preliminary evaluation of changes in the design. Although two-dimensional analysis is adequate to define trends, the accompanying plane stress assumption and imprecise representation of broach geometry do not produce highly accurate stress predictions. Figure 3 shows the finite-element model with which the process began. The modeling method is similar to the three-dimensional approach in the sense that a slice of the disk containing a single blade was isolated for study. The radial sides were assumed to bound a region typical of the 31 cyclically symmetric regions around the disk. This region was sliced normal to the axis of rotation, at the disk mid-plane (Fig. 3) and at the disk rim aft face.

The contact surfaces of the blade and disk each were represented by a line of three equally spaced nodes. The boundary conditions imposed on the contact nodes permitted relative motion between blade and disk along the contact surface. The cyclosymmetric boundary condition was applied along the radial sides, constraining the boundary nodes to the same radial and tangential displacements as their counterparts on the opposite boundary. Displacement boundary conditions

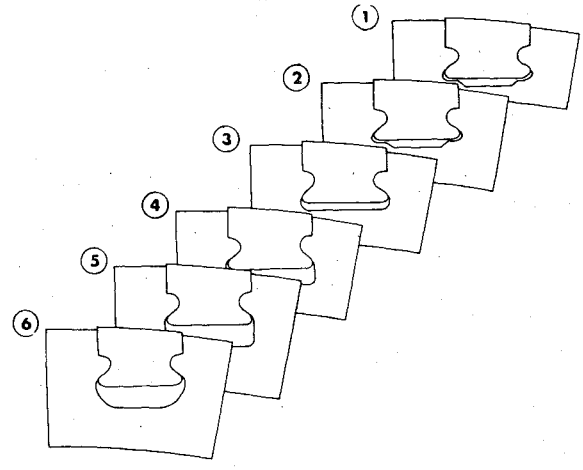

Fig. 4 Broach profiles considered in two-dimensional study.

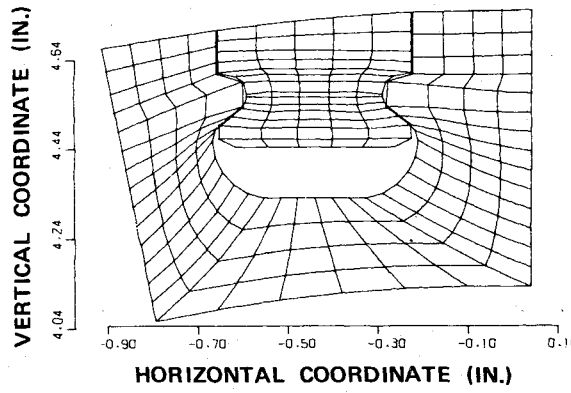

Fig. 5 Two-dimensional finite-element grid of final configuration at rim aft face.

were impressed at the inside radius, based on displacement obtained from analysis of the basic three-dimensional model. The effect of airfoil centrifugal loading was included through force boundary conditions at the upper boundary of the simulated blade. The nodal loads were obtained from the stress distribution calculated with use of the three-dimensional model.

Six configurations (Fig. 4) were examined in the two-dimensional investigation, beginning with the basic configuration and progressing to a configuration that appeared sufficiently promising for three-dimensional analysis. In the basic configuration (Fig. 3), it can be seen that the disk broach conforms to the blade dovetail except at the bottom, where the disk is notched to receive a retaining clip for the blade. The two-dimensional configuration variations that were studied included removal of this notch, since it was likely that the final disk configuration would feature a deeper broach with more generous radii and that a different method of blade retention would have to be employed.

The six steps in the two-dimensional variation study are listed. Each step represents a changed configuration from the preceding case: 1) basic configuration, 2) thicker live rim, 3) remove lips for retaining clip, 4) deeper broach, 5) additional live rim thickness and broach depth, and 6) increased radius in disk broach (final configuration). Grid topology is essentially the same in each case as that shown in Fig. 3. Models representing the slice at the rim aft face do not require any representation of the disk web. Figure 5 shows this model for the final configuration.

The limitations of a two-dimensional finite-element analysis of rim sections with inserted blades have been established from prior correlation studies featuring static pull tests of 5 × -scale aluminum models. In this test program, brit-

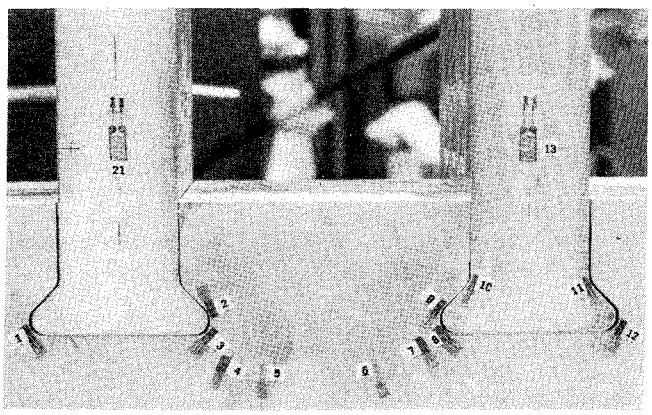

Fig. 6 Pull-test arrangement for simulated blade-disk attachment (aluminum 5×-scale, 0° broach angle).

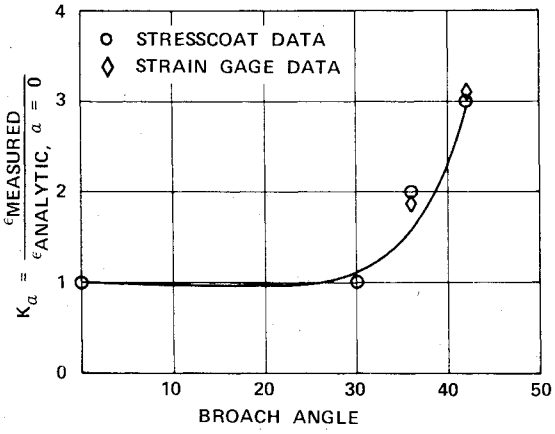

Fig. 7 Comparison of analytical and experimental results from 5×-scale aluminum model.

tle lacquer stress-coat and strain-gage methods were employed. Figure 6 shows one configuration (zero broach angle) with strain gages in place. A series of tests was conducted for models of various broach angles. Results were compared with analytical data generated from a model similar to the one employed in this study. Figure 7 summarizes results from the disk fillet area. Stress-coat and strain-gage results are consistent, and agreement with the two-dimensional analysis is good up to a broach angle of 30°. At 38°, the broach angle employed in this study, analysis understates the fillet strain by a factor of two. The analytical results have been corrected for axial load distribution determined from the testing, so the results shown are about the best that can be expected from two-dimensional analysis. The good agreement at less severe broach angles appears to validate the use of two-dimensional analysis to study trends, however.

III. Results

Three-Dimensional Study of Basic Configuration

The three-dimensional model shown in Fig. 1 was analyzed for a rotational speed of 20,688 rpm. Figure 8 shows magnified displacements in a three-dimensional view of the model. A combined airfoil lean and untwist can be observed. Figure 9 is a display showing details of the three-dimensional effective stress field in the disk. Data have been plotted on a series of five planes normal to the axis of rotation. The figure shows that the highest effective stresses are in opposite fillets at the end faces. Rim thickness is minimum near these fillets. A double stress concentration is also present, because of the fillet radius in the Y-Z plane and the broach angle in the X-Y plane. Individual stress figures of interest are shown in Table 1. The designations "left" and "right" refer to a view of the disk from aft (X positive) looking forward (X negative).

Table 1 Stress summary from three-dimensional analysis: basic configuration

	Maximum effective stress (ksi)		
X	Left fillet	Center of broach	Right fillet
+0.56	42	113	141
+0.28	56	98	99
0	75	81	72
−0.28	104	88	66
−0.56	117	107	38

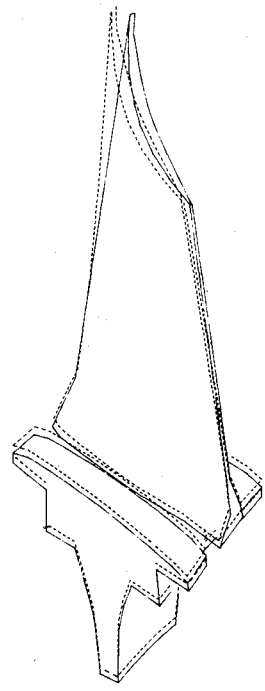

Fig. 8 Magnified displacement of model: basic configuration.

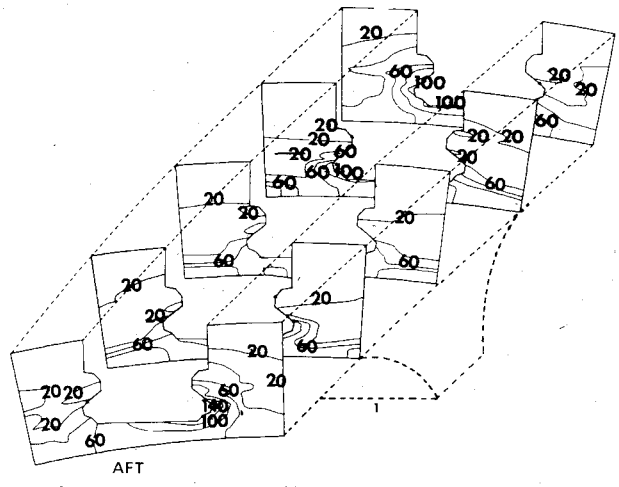

Fig. 9 Three-dimensional effective disk stress distribution: basic configuration.

Figure 10 is a similar presentation for blade shank stress distribution. The areas of highest stress match those of the disk. Figure 11 shows the effective stress distribution on the pressure side of the airfoil. The maximum effective stress (46 ksi) results from the combined effects of centrifugal loading and blade untwist.

Many disk and blade attachments have been designed based on some assumed load distribution on the contact surface. No such assumption is required in a full three-dimensional

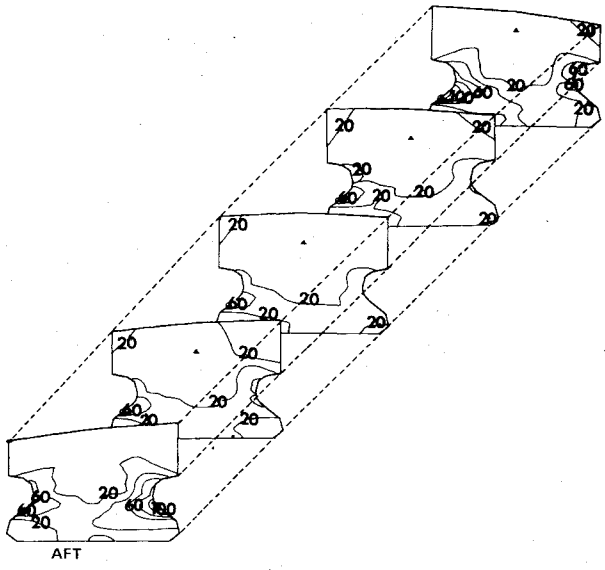

Fig. 10 Three-dimensional effective blade stress distribution: basic configuration.

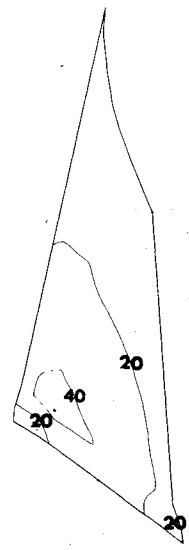

Fig. 11 Effective stress distribution on airfoil pressure side.

analysis. Figure 12 is presented to indicate the load distribution calculated by Program ISO3DQ. The global forces at the 15 nodes that model each contact surface were converted to pressure normal to the surface. The pattern of peak stresses at the acute corners in the disk slot and the adjacent blade shown in Figs. 9 and 10 appear to be influenced more by disk geometry than blade load axial distribution. The distribution of load along the contact surfaces was more uniform that expected. From surface to surface, in Fig. 12, it would appear that a restacking would improve load distribution, but it is apparent from the stress distribution (Fig. 9) that restacking could produce a worse stress pattern.

Some areas of negative load are present. This is because of the nature of the boundary conditions at the contact surface, as discussed earlier. This anomaly can be avoided only with the development of more advanced boundary condition techniques.

Although variations normal to the broach are most striking, it should also be noted that significant variations exist along the broach. Information of this type is not available from two-dimensional analysis.

Two-Dimensional Study

Six different configurations were considered in the progression from the basic to final. Details of the broach and rim geometry are compared in Fig. 4. The profiles shown are a slice of the aft rim face, viewed from the disk aft side, looking forward.

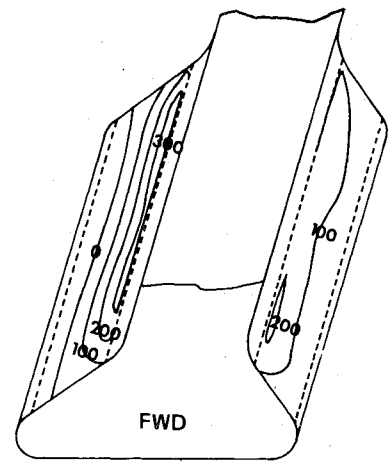

Fig. 12 Pressure distribution (ksi) on contact surface: basic configuration.

Boundary conditions for the six configurations analyzed were similar. For the disk midplane two-dimensional analysis, an inner rim radial displacement of 0.014 in. was specified; at the rim aft face, 0.015 in. was specified. These values were obtained from the three-dimensional analysis of the basic configuration. The rotational speed was 20,688 rpm. Simulated blade loading was obtained by integrating and discretizing platform normal stresses obtained from the three-dimensional analysis.

Table 2 Effective stress summary from two-dimensional analysis

Steps in configuration development	Stress (ksi) at disk midplane			Stress (ksi) at rim aft face			
	Left fillet	Center of broach	Right fillet	Left fillet	Center of broach	Right fillet	Nominal rim thickness, in.
1) Basic	104	77	95	100	97	120	0.05
2) Thicker live rim	104	77	95	97	90	110	0.15
3) Remove lips for retaining clip	103	63	98	92	71	124	0.15
4) Deeper broach	107	63	101	93	74	131	0.10
5) Additional live rim thickness and broach depth	100	64	94	88	73	119	0.20
6) Increased radius in disk broach (final configuration)	89	70	87	85	75	103	0.20

Configuration No. 1 is the basic design, for which the broach conforms closely to the dovetail attachment except for the slot in the bottom of the broach. The nominal rim thickness is 0.05 in., defined as the difference in radial distance from the axis of rotation to the rim inner surface and to the center point in the bottom of the broach. The true rim thickness changes along the circumference because of the relative orientation of the straight broach and the cylindrical rim.

The character of the stress distribution is similar for the various configurations analyzed during this phase of the investigation. Comparative results are presented in Table 2. Reference to the table shows that the maximum fillet stress is significantly higher at the rim aft face than at the midplane. This is because of the lack of disk support in this area.

Configuration No. 2 featured a thicker live rim. An increase in nominal thickness to 0.15 in. reduced the maximum stress to 110 ksi. This modification was chosen as the first step in order to accommodate subsequent changes that would involve material removal. For Configuration No. 3, a smoother broach was achieved by removing the lips for the retaining clip. Analysis of this configuration produced a higher maximum effective stress (124 ksi). Evidently, removal of the lip material brought the fillet under greater influence from the rim tangential stress, and increased effective stress resulted.

Configuration No. 4 featured a deeper broach, a feature that would permit a better surface-finishing operation in the fillet. This modification reduced the nominal rim thickness to 0.10 in. and further increased the maximum effective stress to 131 ksi. Comparisons of results from Configuration No. 1 with No. 2, and No. 3 with No. 4, indicate that changing the nominal rim thickness by 0.01 in. produces about 1 ksi change in maximum effective stress.

Configuration No. 5 utilized this effect by combining additional rim thickness with additional broach depth, which resulted in a nominal rim thickness of 0.20 in. The trend persisted, with maximum effective stress being reduced to 119 ksi. The deeper broach was included in preparation for Configuration No. 6, which included a more generous fillet radius. This further reduced the maximum effective stress to 103 ksi, a decrease of 14% with respect to the basic configuration. Examination of stress data shows that radial and tangential stresses are in the ratio of 1:5 at the point of highest effective stress. For the basic configuration, this ratio was 1:1. Evidently the modifications have removed most of the influence of the fillet and have produced a situation dominated by the hoop stress in the live rim. Configuration No. 6 was considered to show sufficient improvement to be examined with a three-dimensional model.

Three-Dimensional Analysis of Final Configuration

Based on the broach contour developed in the two-dimensional studies, a three-dimensional model was constructed and analyzed. This model differed from the basic model in rim width also, but the general characteristics of the stress distribution are like those for the basic configuration. Table 3 summarizes the effective stress data, and should be compared to Table 1 data to see the overall effect of the modification. An improvement of 13% was realized. For the environment in which this disk operates, the improvement would increase low-cycle-fatigue life almost 100%.

Comparison of results from two- and three-dimensional analyses supports the contention that two-dimensional analysis is a valuable method for establishing trends but can lack sufficient accuracy to predict stress magnitudes. This is seen by comparing stresses from Tables 1, 2, and 3. Both two- and three-dimensional analyses predict an improvement of about the same percentage because of the modification, but the maximum effective stresses predicted for the final configuration by the two methods differ by about 20%.

Table 3 Stress summary from three-dimensional analysis: final configuration

	Maximum effective stress (ksi)		
X	Left fillet	Center of broach	Right fillet
+0.78	51	93	121
+0.39	63	86	81
0	72	86	73
−0.39	81	87	61
−0.78	121	90	46

IV. Conclusions

A practical approach to the design of a disk and blade attachment has been demonstrated, combining the accuracy of three-dimensional analysis with the economy of two-dimensional analysis. Analysis in three dimensions is obviously a costly process (approximately 50 times longer than a single two-dimensional analysis), but it appears that an accurate definition of the stress distribution in a complex three-dimensional component can be obtained in no other way. Variations in contact load, the axial distribution of stress, and the effect of broach-angle variation are not available from two-dimensional analysis. Continued use of two-dimensional analysis is recommended, however, to establish trends resulting from variations in the broach geometry.

References

[1] Tree, D. J., Harvey, J. W., and Tani, M. A., "User's Manual – Program ISOPDQ," AiResearch Mfg. Co., Rep. No. 74-210860 (2), July 1974.

[2] Ergatoudis, I., Irons, B. M., and Zienkiewicz, O. C., "Curved Isoparametric Quadrilateral Elements for Finite Element Analysis," *International Journal of Solids and Structures,* Vol. 4, Jan. 1968, pp. 31–42.

[3] Oden, J. T. and Brauchli, H. J., "On the Calculation of Consistent Stress Distributions in Finite Element Approximations," *International Journal for Numerical Methods in Engineering*, Vol. 3, July-Sept. 1971, pp. 317-325.

[4] Wempner, G. A., Oden, J. T., and Kross, D. A., "Finite Element Analysis of Thin Shells," *Journal of the Engineering Mechanics Division*, American Society of Civil Engineers, Dec. 1968, pp. 1273-1294.

[5] Doherty, W. P., Wilson, E. L., and Taylor, R. C., "Stress Analysis of Axisymmetric Solids Utilizing Higher-Order Quadrilaterial Finite Elements," Structural Engineering Laboratory, Univ. of Calif., Rep. No. 69-3, Jan. 1969.

[6] Zienkiewicz, O. C., Taylor, R. L., and Too, J. M., "Reduced Integration Technique in General Analysis of Plates and Shells," *International Journal for Numerical Methods in Engineering*, Vol. 3, April-June 1971, pp. 275-290.

[7] Pawsey, S. F., and Clough, R. W., "Improved Numerical Integration of Thick Shell Finite Elements," *International Journal for Numerical Methods in Engineering,* Vol. 3, Oct.-Dec. 1971, pp. 575-586.

[8] Greene, B. C., "Application of Generalized Constraints in the Stiffness Method of Structural Analysis," *AIAA Journal,* Vol. 4, Sept. 1966. pp. 1531–1537.

[9] Pian. T.H.H., "Derivation of Element Stiffness Matrices," *AIAA Journal,* Vol. 2, March 1964, pp. 576–577.

[10] Anderheggen, E., "A Conforming Triangular Finite Element Plate Bending Solution," *International Journal for Numerical Methods in Engineering*, Vol. 2, April-June 1970, pp. 259-264.

[11] Harvey, J. W. and Kelsey, S., "Triangular Plate Bending Elements with Enforced Compatibility," *AIAA Journal*, Vol. 9, June 1971, pp. 1023–1026.